Pharmaceutical Research, Vol. 22, No. 12, December 2005 (© 2005)
DOI: 10.1007/s11095-005-8112-0

Research Paper

Quantitative Structure–Activity Relationship and Quantitative Structure–Pharmacokinetics Relationship of 1,4-Dihydropyridines and Pyridines as Multidrug Resistance Modulators

Xiao-Fei Zhou,[1] Qingxiang Shao,[2] Robert A. Coburn,[3] and Marilyn E. Morris[1,4]

Received December 23, 2004; accepted August 16, 2005

Purpose. The aim of this study was to develop quantitative structure–activity/pharmacokinetic relationships (QSAR/QSPKR) for a series of synthesized 1,4-dihydropyridines (DHPs) and pyridines as P-glycoprotein (P-gp) inhibitors.
Methods. Molecular descriptors of test compounds were generated by 3D molecular modeling using SYBYL and KowWin programs. Forward inclusion coupled with multiple linear regression (MLR) was used to derive a QSAR equation for Ca^{2+} channel binding. A multivariate statistical technique, partial least square (PLS) regression, was applied to derive a QSAR model for P-gp inhibition and QSPKR models. Cross-validation using the "leave-one-out" method was performed to evaluate the predictive performance of models.
Results. For Ca^{2+} channel binding, the MLR equation indicated a good correlation between observed and predicted values ($R^2 = 0.90$), and cross-validation confirmed the predictive ability of the model ($Q^2 = 0.67$). For P-gp reversal, the model obtained by PLS could account for most of the variation in P-gp inhibition ($R^2 = 0.76$) with fair predictive performance ($Q^2 = 0.62$). Nine structurally related 1,4-DHP drugs were used for QSPKR analysis. The models could explain the majority of the variation in clearance ($R^2 = 0.90$), and cross-validation confirmed the prediction ability ($Q^2 = 0.69$).
Conclusion. QSAR/QSPKR models were developed, and the QSAR models were capable of identifying synthesized 1,4-DHPs and pyridines with potent P-gp inhibition and reduced Ca^{2+} channel binding. The QSPKR models provide insight into the contribution of electronic, steric, and lipophilic factors to the clearance of DHPs.

KEY WORDS: dihydropyridines (DHPs); multidrug resistance (MDR); P-glycoprotein (P-gp); quantitative structure–activity relationship (QSAR); quantitative structure–pharmacokinetic relationship (QSPKR).

[1] Department of Pharmaceutical Sciences, University at Buffalo, State University of New York, 517 Hochstetter Hall, Amherst New York 14260-1200, USA.
[2] Department of Clinical Pharmacology, Zhejiang Academy of Medical Sciences, Hangzhou 310013, China.
[3] Department of Chemistry, University at Buffalo, State University of New York, Amherst New York 14260, USA.
[4] To whom correspondence should be addressed. (e-mail: memorris@buffalo.edu)

ABBREVIATIONS: 1,4-DHPs, 1,4-dihydropyridines; CL, clearance; COAR, Connolly surface area; COCO, core–core repulsion; COVO, Connolly surface volume; DNM, daunomycin; ELEN, electronic energy; FILE, filled levels; HEFO, heat of formation; HOMO, energy of the highest occupied molecular orbital; IOPO, ionization potentials; LUMO, energy of the lowest unoccupied molecular orbital; MDR, multidrug resistance; MLR, multiple linear regression; MW, molecular weight; P-gp, P-glycoprotein; PLS, partial least square; PSA, polar surface area; QSAR, quantitative structure–activity relationship; QSPKR, quantitative structure–pharmacokinetic relationship; TOEN, total energy of the molecule; V, apparent volume of distribution; VBL, vinblastine.

INTRODUCTION

Multidrug resistance (MDR) remains a serious limitation to successful chemotherapy in metastatic cancers. It is believed that overexpression of P-glycoprotein (P-gp), a 170-kDa efflux pump, is associated with insufficient accumulation of anticancer drugs into tumor cells (1). A large number of structurally diverse compounds have been identified as MDR modulators, which can reverse drug efflux mediated by P-gp. 1,4-Dihydropyridines (DHPs) have affinity for P-gp at a site that allosterically interacts with other drug acceptor sites (2). Therefore, 1,4-DHPs emerged as good drug candidates and became the most extensively investigated compounds as P-gp reversal agents (3). 1,4-DHPs are also well known as calcium channel blockers, and the major setback to the use of 1,4-DHPs as clinical MDR modulators is the dose-limiting cardiovascular toxicity (4).

Recently, 3D molecular modeling has been applied to develop quantitative structure–activity relationship (QSAR)

models of structurally related drugs with MDR modulating activity (5,6). In these studies, conformational profiles of compounds were investigated to obtain insight into which conformations are involved in the interaction with biological targets. Furthermore, with the application of multivariate statistical analysis, quantitative structure–pharmacokinetics relationship (QSPKR) models were also developed based on various molecular physicochemical descriptors generated by 3D modeling software (7). The purpose of this study was to develop QSAR for 1,4-DHPs and pyridines based on 3D molecular descriptor methods and to identify 1,4-DHPs and pyridines with potent P-gp inhibition and reduced toxicity (Ca^{2+} channel binding). Furthermore, the pharmacokinetic parameters (clearance and volume of distribution) of the newly synthesized compounds were also predicted based on multivariate QSPKR analysis to identify compounds with suitable pharmaceutical properties for further evaluation.

MATERIALS AND METHODS

Chemicals

Compounds I_a–I_q and II_a–II_p were synthesized in Professor Robert Coburn's laboratory, Department of Chemistry, University at Buffalo. The chemical structures of these newly synthesized compounds are shown in Fig. 1, and the synthesis is described in a recent publication (8).

P-gp Inhibition and Pharmacokinetic Data

The determination of the inhibition constant K_i for Ca^{2+} channel binding was conducted using rat cerebral cortex membrane preparations. The K_i values were obtained from the literature (9) for the following selected 1,4-DHP Ca^{2+}

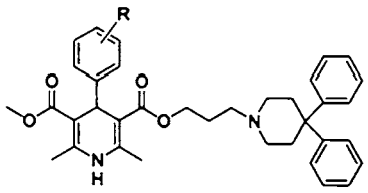

I

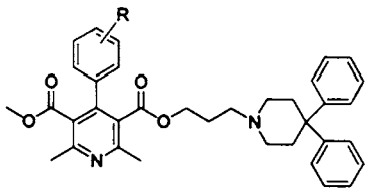

II

Series I Compound	R	Series II Compound	R
I_a	3-NO_2	II_a	3-NO_2
I_b	4-OMe	II_b	4-OMe
I_c	4-OEt	II_c	4-OEt
I_d	4-NMe_2	II_d	4-NMe_2
I_e	4-OBn	II_m	4-OMe, 3-OMe
I_g	4-OCOMe	II_n	3,4-OCH_2CH_2O
I_j	4-OH	II_o	3,4-OCH_2O-
I_k	3-OH	II_p	4-O^nPr
I_l	4-OH, 3-Me		
I_m	4-OMe, 3-OMe		
I_n	3,4-OCH_2CH_2O		
I_o	3,4-OCH_2O-		
I_q	4-O^nBu		

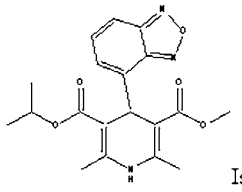

Isradipine

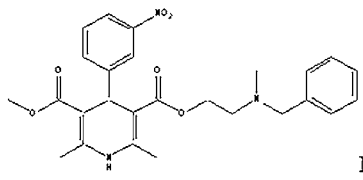

Nicardipine

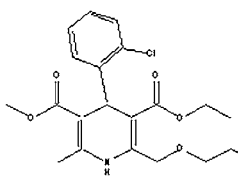

Amlodipine

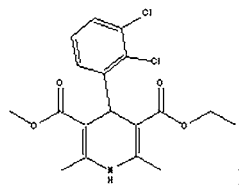

Felodipine

Fig. 1. Chemical structures of newly synthesized 1,4-dihydropyridines (I), 4-aryl-pyridines (II), and selected calcium channel blockers.

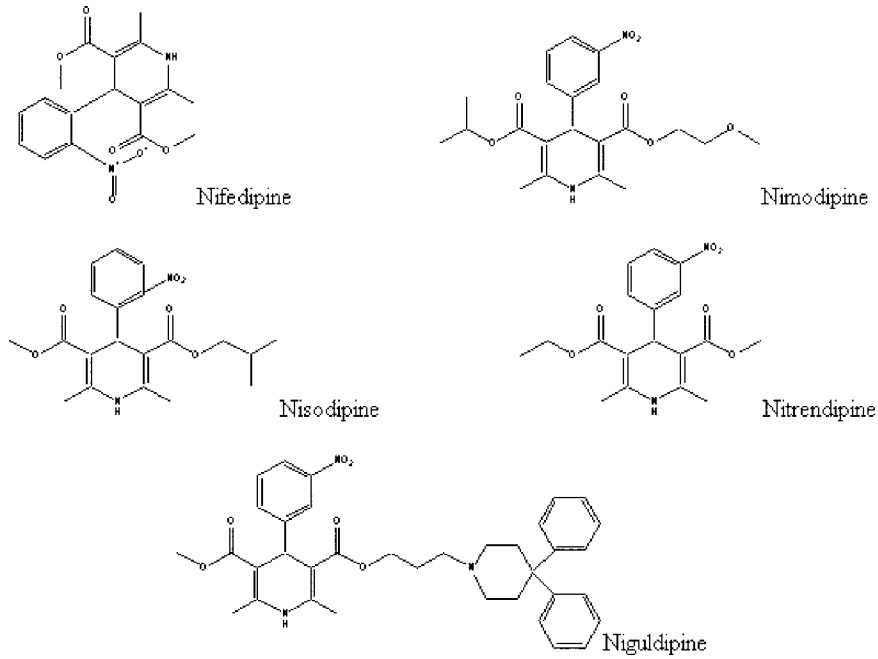

Fig. 1. Continued.

channel blockers: isradipine, nicardipine, amlodipine, felodipine, nifedipine, nimodipine, nisodipine, and nitrendipine.

The P-gp modulation effect of the newly synthesized compounds were evaluated by [^{3}H]vinblastine (VBL) accumulation and daunomycin (DNM) cytotoxicity studies in MCF-7/adr cells, which are resistant human breast cancer cells. P-gp reversal activity was characterized using the log(MDR ratio) and IC_{50} of DNM cytotoxicity. MDR ratio is the percentage increase of VBL accumulation compared to the vehicle control. The pharmacokinetic data of selected compounds were obtained from the literature (10,11).

Molecular Modeling

Compound structures were sketched in a Silicon Graphic workstation using SYBYL molecular modeling software (Tripos, Inc., version 6.7, St. Louis, MO, USA). Charges within compounds were calculated using the Gasteiger method. The energy minimization was initially carried out based on both electrostatic and steric components using Tripos force field minimizer (MAXMIN 2) to gradient convergence (criteria used: gradient energy change, 0.01 kcal/Å; rms displacement, 0.001 Å; nonbonded cutoff, 8.000 Å; dielectric function, distant dependent; dielectric constant, 1.00), followed by MOPAC AM1 geometry optimization.

Thirteen physicochemical descriptors were generated by SYBYL molecular modeling software. These descriptors were calculated by the MOPAC module in SYBYL using the Austin Model 1 (AM1) singlet method with the *precision* option activated and a time limit of 1 h for convergence. LogP was calculated by KowWin program (Syracuse Research Corporation, Syracuse, NY, USA).

The electronic descriptors include heat of formation, filled levels, energy of the lowest unoccupied molecular orbital, energy of the highest occupied molecular orbital, electronic energy, total energy of the molecule, and ionization potentials. Four steric descriptors were calculated in the present study, namely, core–core repulsion, molecular weight, polar surface area, Connolly surface area, and Connolly surface volume. The Connolly surface area (solvent accessible area) is defined as the area a theoretical water molecule (1.4 Å in diameter) produces when it moves over the van der Waals surface of a ligand.

Data Analysis

An automatic forward stepwise inclusion method combined with multiple linear regression (MLR) was applied to derive a QSAR model for Ca^{2+} channel binding. The descriptor entry and exit tests were considered significant at an $\alpha = 0.05$. The predictive performance of the final model was tested by cross-validation using the "leave-one-out" method (7,12). Briefly, a statistical model is redeveloped with a compound removed from the dataset. Subsequently, the model is used to predict the biological target of the removed compound (Y_{pred}). The process is repeated until each compound in the dataset is removed and predicted once. The cross-validated R^2, also called Q^2, is calculated according to the following equation:

$$Q^2 = 1 - \sum (Y_{pred} - Y_{obs})^2 \Big/ \sum (Y_{pred} - Y_{mean})^2 \qquad (1)$$

A model with good internal predictive performance will have Q^2 value close to 1. A Q^2 with a negative value indicates chance correlations.

Partial least square (PLS) regression is a multivariate statistical method that is widely applied in the QSAR area. In contrast to MLR, PLS can deal with the situation when the number of descriptors is greater than the number of compounds/observations and colinearity between the descriptor variables. PLS is also likely to be a robust method when a dataset is ill-conditioned (13). In this study, PLS

regression was applied to develop QSPKR models and QSAR analysis for P-gp inhibition. Cross-validation using "leave-one-out" was also performed to evaluate the predictive ability of models.

All MLR and PLS calculations were performed using the SAS statistical package (version 8.2, SAS Institute Inc., Cary, NC, USA).

RESULTS

Generation of Molecular Descriptors

A summary of molecular descriptors calculated by SYBYL and KowWin computer programs is listed in Table I. Lipophilicity has been long viewed as an important factor in QSAR/QSPKR analysis. Among the several different methods for estimating LogP values of these compounds, the KowWin method was employed based on the superior performance of this method in experimental studies reported by Meylan and Howard (14), who checked the validity of LogP calculations for the substructure method KowWin and the whole-molecule approach SciLogP by comparing the values with the experimental LogP determined for a set of 180 molecules, composed of 90 simple organics and 90 more complex drug molecules. On the basis of the averaged absolute residual sums, the superiority of KowWin to SciLogP was observed for the entire dataset (14).

QSAR for Ca^{2+} Channel Binding

The calcium channel binding activities for the 14 compounds that exhibited quantifiable activity are listed in Table II and included in the QSAR analysis for Ca^{2+} channel binding. All other compounds tested had negligible activity in this assay. The final QSAR equation for calcium channel binding can be expressed as follows:

$$\log 1/K_i = -0.0000453 * \mathrm{COCO} + 0.163 * \mathrm{DIPO} + 9.484 \quad (2)$$
$$\left(R^2 = 0.90,\ Q^2 = 0.67,\ n = 14\right)$$

This MLR model for Ca^{2+} channel binding indicated a good correlation between the predicted and observed data (R^2 = 0.90) and fair predictive performance (Q^2 = 0.67). It seems that core–core repulsion, a steric factor reflecting the geometry (bond length, angles, etc.) of a molecule, and dipole moment are highly associated with the Ca^{2+} channel binding activity of a compound. The relationship between the predicted and observed $\log(1/K_i)$ is illustrated in Fig. 2.

Table I. Physicochemical Descriptors of 1,4-DHPs and 4-Aryl-Pyridines

Compound	HEFO	DIPO	IOPO	MW	COAR	COVO	LUMO	HOMO	LogP	TOEN	COCO	FILE	ELEN	PSA
I_a	−64.63	4.24	9.02	609.7	574.1	620.2	−0.82	−9.02	6.84	23.28	67,737	117	−75,422	135.2
I_b	−104.9	4.7	8.64	594.7	579.8	626.3	−0.37	−8.64	7.10	21.61	65,026	115	−72,357	65.68
I_c	−97.2	4.57	8.61	608.8	600.3	644.9	−0.35	−8.61	7.59	21.68	67,432	118	−74,918	59.8
I_d	−56.82	2.89	8.12	697.8	599.1	651.0	−0.25	−8.12	7.20	25.27	67,884	118	−75,270	54.54
I_e	−28.21	3.85	8.44	670.8	630.8	718.1	−0.14	−8.44	8.81	19.98	78,769	129	−86,920	61.18
I_g	−144.4	2.71	8.73	622.8	603.9	648.2	−0.41	−8.73	6.62	22.36	69,440	120	−77,219	81.86
I_j	−89.4	4.91	8.74	580.7	561	607.1	−0.41	−8.74	6.54	20.60	62,589	112	−69,764	106.2
I_k	−110.9	4.27	8.81	580.7	560.3	606.9	−0.42	−8.81	6.54	20.60	62,996	112	−70,172	106.2
I_l	−118.4	4.92	8.64	594.7	577.8	626.3	−0.39	−8.64	7.09	21.50	65,252	115	−72,583	99.9
I_m	−139.8	4.33	8.77	624.8	600.7	630.5	−0.44	−8.77	6.66	22.50	71,118	121	−78,925	63.4
I_n	−147.6	5.12	8.77	622.8	591.3	636.8	−0.43	−8.77	6.78	21.24	70,129	120	−77,908	83.9
I_o	−125.9	4.32	8.62	608.7	574.5	623.4	−0.46	−8.62	7.08	33.50	67,235	117	−74,858	92.5
I_q	−124.1	4.62	8.61	636.8	639.4	683.4	−0.36	−8.61	8.57	22.60	71,979	124	−79,778	58.46
II_a	−50.9	7.58	9.27	607.7	570.2	615.1	−1.11	−9.27	7.49	17.00	66,887	116	−74,544	122.2
II_b	−94.8	1.68	9.11	592.7	576.8	618.8	−0.59	−9.11	7.75	16.90	64,841	114	−72,144	50.5
II_c	−100.2	1.95	9.07	606.8	597.5	637.3	−0.57	−9.07	8.24	16.99	67,186	117	−74,645	42.49
II_d	−48.2	3.61	8.38	605.8	593.8	642.6	−0.48	−8.38	7.85	20.50	67,627	117	−74,986	39.6
II_m	−119.3	5.05	9.29	622.8	590.5	651.4	−0.98	−9.29	7.32	24.80	72,726	120	−80,504	97.2
II_n	−136	3.76	9.22	620.7	588.1	634.5	−0.67	−9.22	7.72	16.60	69,874	119	−77,625	65.7
II_o	−114.8	1.3	9.07	606.7	572.9	613.7	−0.68	−9.07	7.73	29.00	67,293	116	−74,888	74.9
II_p	−107.1	4.31	9.05	620.8	600.9	660.5	−0.58	−9.05	8.73	16.23	70,810	120	−78,424	49.63
Isradipine	−7.36	10.11	8.60	371.4	339.5	368.6	−1.92	−8.60	3.48	24.51	33,789	71	−38,728	142.7
Nicardipine	−91.0	12.3	9.1	493.6	471.4	495.6	−0.72	−9.1	3.90	18.17	49,561	95	−55,985	129.8
Amlodipine	−111.4	2.6	9.33	422.9	372.5	438.9	−0.18	−9.33	2.07	6.30	41,389	79	−46,837	131.1
Felodipine	−133.1	7.34	8.72	384.3	339.0	361.3	−0.22	−8.72	4.46	9.56	30,483	67	−35,285	47.87
Nifedipine	−111.4	2.75	8.85	346.3	301.3	327.6	−0.54	−8.8	2.50	13.04	31,070	66	−35,827	100.1
Nimodipine	−168.9	6.44	9.04	418.4	403.7	413.9	−0.86	−9.04	3.13	14.90	41,420	81	−47,121	132.5
Nisodipine	−111.1	9.6	8.15	389.4	326.9	397.6	−4.91	−8.94	3.90	11.80	37,393	75	−42,630	104.3
Nitrendipine	−58.1	8.7	9.94	360.4	332.2	352.2	−1.06	−9.94	2.99	13.40	32,382	69	−37,293	156.4

DHPs, Dihydropyridines; HEFO, heat of formation; FILE, filled levels; LUMO, energy of the lowest unoccupied molecular orbital; HOMO, energy of the highest occupied molecular orbital; ELEN, electronic energy; TOEN, total energy of the molecule; IOPO ionization potentials; COCO, core–core repulsion; MW, molecular weight; PSA, polar surface area; COAR, Connolly surface area; COVO, Connolly surface volume.

Table II. Calcium Channel Binding Activity Values for the Test Compounds[a]

Compound	K_i (nM)	log(1/K_i)
I_e	157.3	6.80
I_g	287.9	6.54
I_n	310.3	6.51
I_q	102.3	6.99
II_c	56.7	7.25
II_p	74.3	7.13
Israpdipine	0.12	9.92
Nicardipine	1.16	8.94
Amlodipine	24.3	7.61
Felodipine	0.28	9.55
Nifedipine	6.67	8.18
Nimodipine	0.4	9.40
Nisodipine	0.4	9.40
Nitrendipine	0.62	9.21

[a] All other newly synthesized dihydropyridine compounds had negligible calcium channel blocking activity at concentrations as high as 3 μM. Log(1/K_i) values were calculated using K_i values expressed as M concentrations.

QSAR for P-gp Inhibition

Table III shows the results from VBL accumulation and DNM cytotoxicity studies. The results are log-transformed to accommodate the QSAR analysis. For a set of ill-conditioned data, PLS regression represents a good alternative to the more classical MLR and principal component analysis and is likely to result in a more robust predictive model (15). The summary of PLS regression for log(MDR ratio) and log(1/IC_{50}) is shown in Table IV. The PLS model for log(MDR ratio) using the P-gp inhibition data from VBL accumulation studies could account for 62.9% of the variation of the observed values. The model for log(1/IC_{50}) showed fair correlation between the observed and predicted values (R^2 = 0.76). The predictability of this model was evaluated by cross-validation (Q^2_{LogMDR} = 0.40, $Q^2_{Log1/IC50}$ = 0.62), which indicates that the model should be used with caution in estimating log(1/IC_{50}). The relationship between the predicted and observed P-gp modulation effects of compounds from the two studies is shown in Fig. 3.

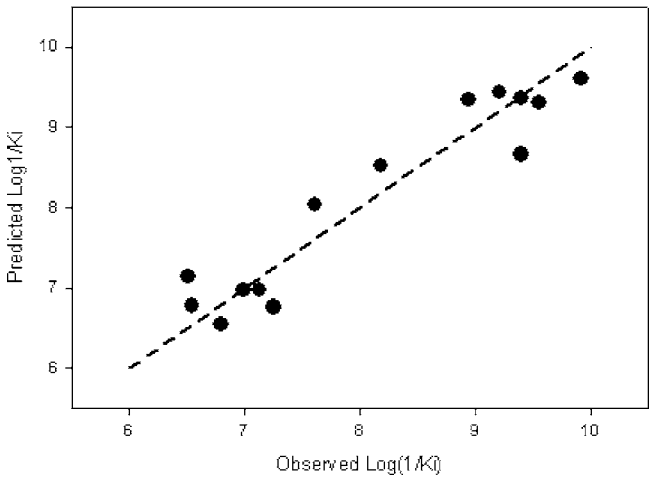

Fig. 2. Relationship between observed and predicted log(1/K_i) (dashed line represents the line of identity).

Table III. Vinblastine Accumulation (log MDR Ratio) and Cytotoxicity (DNM IC_{50}) Values for the Test Compounds

Compound	log(MDR ratio)	log(1/IC_{50})
I_a	0.9593	5.86
I_b	1.0344	5.61
I_c	0.9031	5.48
I_d	0.8555	5.42
I_e	0.8740	5.71
I_g	0.6562	5.72
I_j	0.8212	5.66
I_k	0.9265	5.88
I_l	0.8915	6.40
I_m	1.0944	6.49
I_n	1.0314	6.00
I_o	1.1022	6.00
I_q	1.1360	6.04
II_a	1.0240	6.09
II_b	0.9160	5.66
II_c	1.0987	6.37
II_d	0.9688	5.98
II_m	0.9996	6.15
II_n	0.9796	6.39
II_o	1.0171	5.93
II_p	1.1882	6.28

Log(1/IC_{50}) values were calculated using IC_{50} values expressed as M concentrations.

QSPKR of Selected 1,4-DHPs

Clearance (CL) and volume of distribution (V) values of selected 1,4-DHPs are listed in Table V. QSPKR models, obtained by PLS regression, were built using the 14 molecular descriptors listed in Table I. The results of PLS regression for CL and V are summarized in Table VI. The QSPKR model for volume of distribution can explain nearly 70% variation of the data. Most of variation in clearance can be accounted for by the PLS model (R^2 = 0.90). The predictive performance of PLS model is fair for clearance (Q^2 = 0.69) and relatively poor for V (Q^2 = 0.43). The high values of R^2 and Q^2 for each model indicated model fair predictability and adequate extracted components (16). The relationship between the predicted and observed pharmacokinetic parameters is shown in Fig. 4.

DISCUSSION

1,4-DHPs possess both Ca^{2+} channel blocking and P-gp inhibitory activities. As such, the use of 1,4-DHPs as clinical multidrug resistance modifiers poses therapeutic problems because of their potential vasodilator activity. Based on the results from previous structure–activity relationship studies, a series of 1,4-DHPs and pyridine compounds have been synthesized to increase P-gp reversal and reduce Ca^{2+}

Table IV. Summary of Partial Least Square (PLS) Regression Analysis Using log(MDR Ratio) and log(1/IC_{50})

Properties	No. of components	Q^2	R^2
log(MDR ratio)	6	0.40	0.63
log(1/IC_{50})	6	0.62	0.76

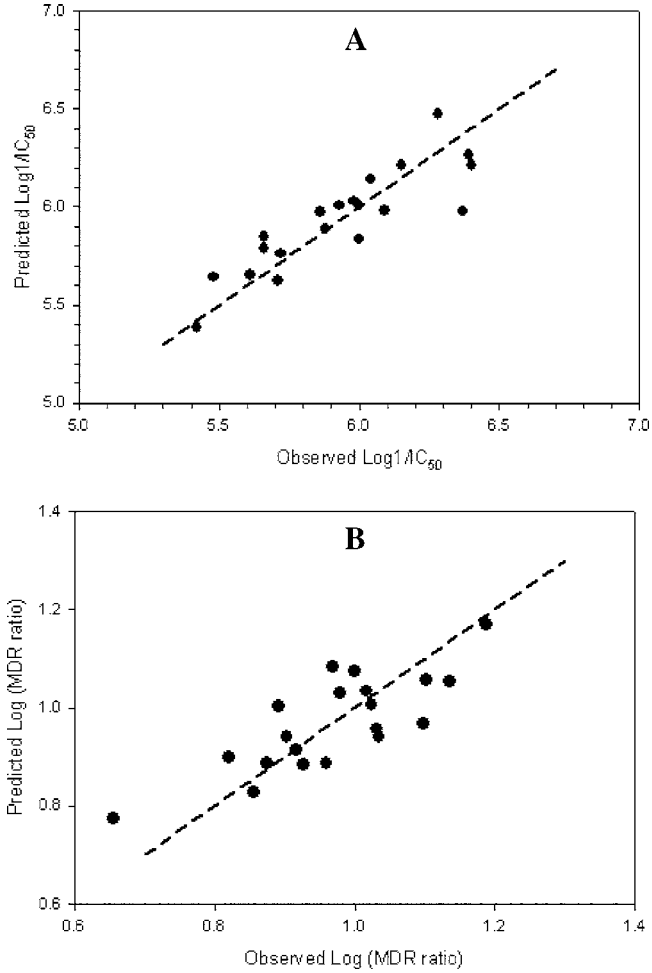

Fig. 3. Relationship between observed and predicted (A) log(1/IC_{50}) and (B) log(MDR ratio) (dashed line represents the line of identity).

channel binding activities. In this study, our purpose was to identify compounds from this series of 1,4-DHPs and pyridines with potent P-gp inhibitory effects, minimal Ca^{2+} channel binding (to reduce potential side effects), and predicted low clearance, based on QSAR/QSPKR prediction models.

1,4-DHPs have been evaluated in several QSAR studies regarding their calcium channel blocking activity (17,18) and P-gp modulation effect (19). Coburn *et al.* (18) found that

Table V. Pharmacokinetic Parameters of Selected 1,4-Dihydropyridine Calcium Channel Blockers

Compound	Clearance (l/h)	*V* (l/kg)
Israpdipine	44.1	70
Nicardipine	0.48	0.275
Amlodipine	0.42	21.4
Felodipine	49.4	9.7
Nifedipine	0.234	0.28
Nimodipine	0.84	0.94
Nisodipine	0.96	2.3
Nitrendipine	2.07	6.6
Dexniguldipine	36.9	17.04

Table VI. Summary of PLS Regression of Clearance and Volume of Distribution of the Selected 1,4-DHPs

PK parameters	No. of components	Q^2	R^2
Clearance	5	0.69	0.90
Volume of distribution	4	0.43	0.70

including steric terms in QSAR equations yielded a good correlation between structure and Ca^{2+} channel binding data for a set of 46 1,4-DHPs. In the present study, core–core repulsion, a steric descriptor indicating the geometry of a molecule (20) (atomic numbers, bond lengths, bond angles, and dihedral angles), has considerable influence in the Ca^{2+} channel binding activity of a compound. The dipole moment also has a significant contribution, which was previously observed in another series of Ca^{2+} antagonists whose dipole properties were shown to play an important role in long-range ligand-receptor recognition and subsequent binding (21). Dipole moments, which are the quantitative measurements of separation of charge, could describe direct drug–receptor interactions between 1,4-DHPs and calcium channels through noncovalent bonding (22).

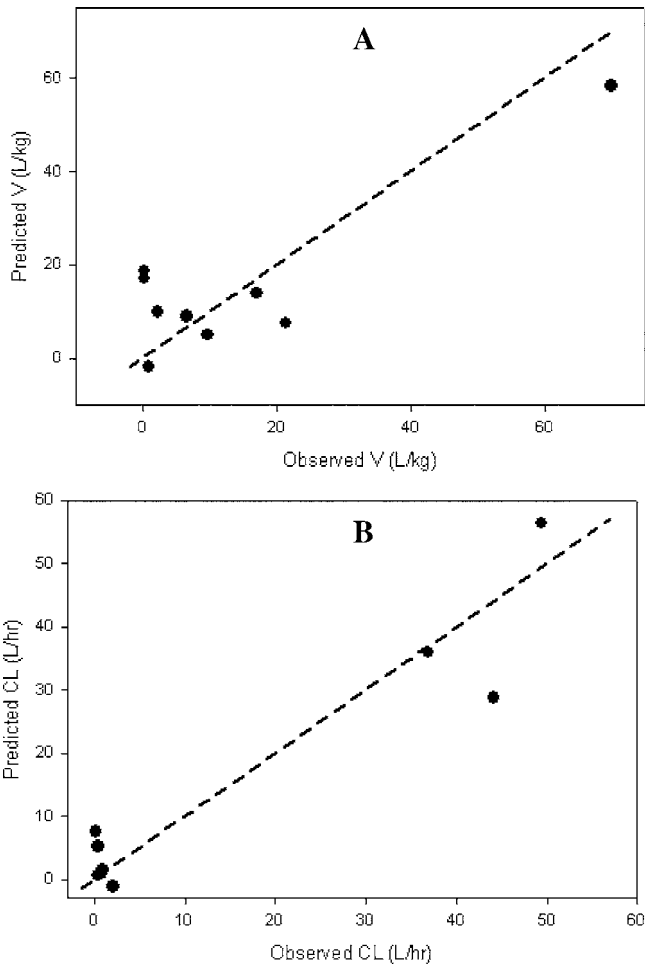

Fig. 4. Relationship between observed and predicted (A) apparent volume of distribution (*V*) and (B) clearance (CL) (dashed line represents the line of identity).

In the QSPKR analysis, the number of predictors (molecular descriptors) exceeds the number of compounds. In this case, ordinary MLR regression would not be suitable for developing meaningful and robust statistical models. Therefore, a multivariate statistical technique, partial least square (PLS) regression, was applied. PLS regression is a relatively new technique that generalizes and combines features from principal component analysis and multiple regression. When the number of predictors exceeds the number of observations (which is often the case in QSAR/QSPKR studies), it is likely to obtain a model that fits the sampled data perfectly but that will fail to predict new data well; this phenomenon is called overfitting. In such cases, although there are many manifest factors, there may be only a few underlying or latent factors (also called components) that account for most of the variation in the response. The goal of PLS is to extract these latent factors, accounting for as much of the manifest factor variation as possible while modeling the response well (13). The optimal number of components in PLS is usually determined by some heuristic technique based on the amount of residual variation. Another approach is to construct the PLS model for a given number of factors on one set of data and then to test it on another, choosing the number of extracted factors for which the total prediction error is minimized (13). Because of the relatively small dataset, the optimal number of PLS components is chosen by the number of components that maximizes Q^2 by leave-one-out cross-validation (7).

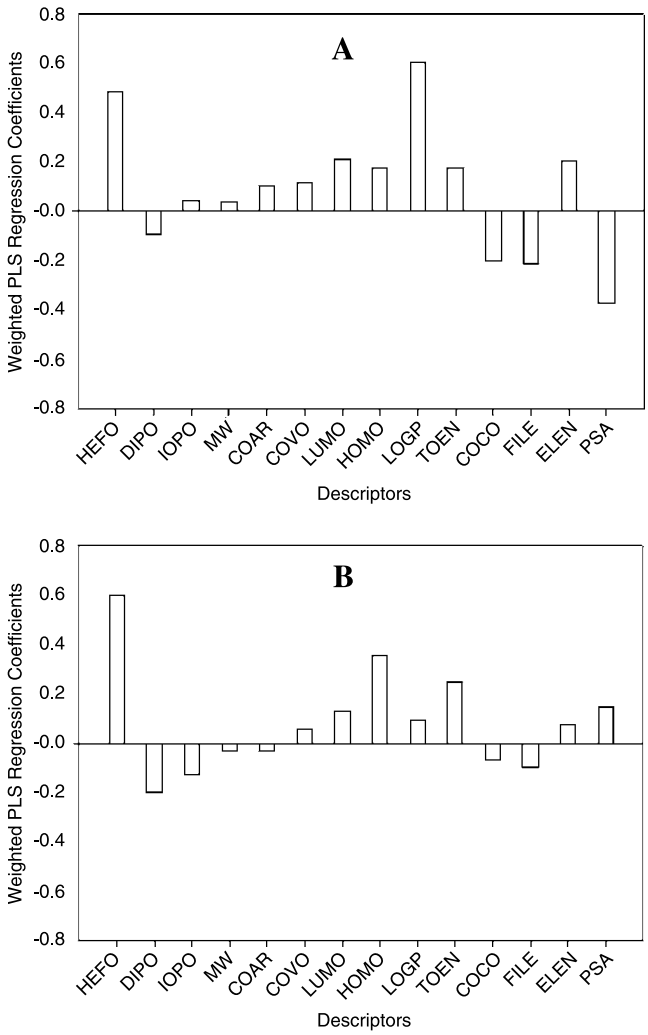

Fig. 5. Weighted partial least square (PLS) regression coefficients for (A) CL and (B) apparent volume of distribution (V).

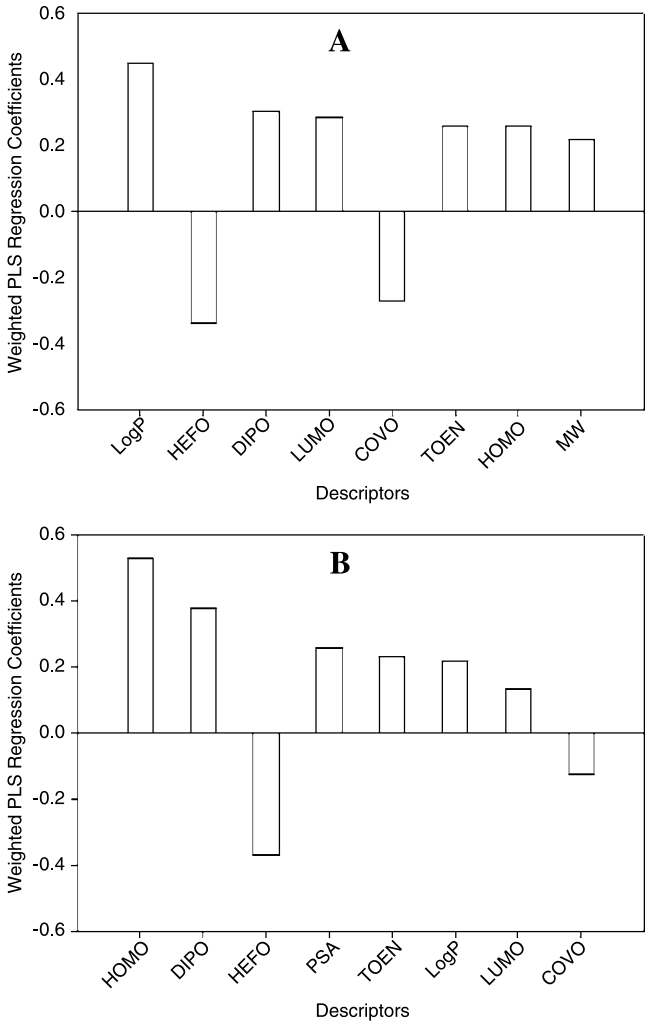

Fig. 6. Weighted PLS regression coefficients for P-gp modulation: (A) $\log(1/IC_{50})$; (B) log(MDR ratio).

The PLS regression models can be expressed in terms of regression coefficients ($\boldsymbol{b}_{PLS}$):

$$\mathbf{Y} = \boldsymbol{X}^{*}\boldsymbol{b}_{PLS} + \mathbf{F}$$

where $\mathbf{Y}$ is the dependent variable matrix (e.g., biological activities), $\boldsymbol{X}$ are the predictors (e.g., molecular descriptors), and $\mathbf{F}$ is the residual matrix. The regression coefficients can be useful in determining the influence of each variable in $\boldsymbol{X}$ in the model (16).

QSPKR models for volume of distribution and clearance can be qualitatively interpreted based on weighted PLS regression coefficients (Fig. 5). LogP and heat of formation were important in the systemic clearance of these compounds. High lipophilicity was associated with high clearance. Polar surface area (the sum of molecular surface of polar atoms, usually oxygens, nitrogens, and attached hydrogens) was inversely related with CL, which is in accordance with

reports that lower polar surface area is associated with greater bioavailability (23,24). The roles of the remaining molecular descriptors were less important in the prediction of clearance. Heat of formation, a descriptor indicating the intrinsic energy of a compound, apparently has high impact on both clearance and apparent volume of distribution, which was also observed in a previous QSPKR study (7). The poor predictive performance of the PLS model for volume of distribution values is likely a result of the limited range of values for *V* for the compounds used in the evaluation.

The results of the QSAR analyses from our two P-gp modulation studies are comparable. Among the 14 descriptors, the 8 leading descriptors, which have relatively high contributions in the two studies, are quite similar based on PLS regression coefficients (Fig. 6). LogP seems to be highly correlated with P-gp inhibitory effect in DNM cytotoxicity (log $1/IC_{50}$). This result is in accordance with the observations from other QSAR studies where the role of lipophilicity of a compound in MDR reversal activity was reported (6,25). The QSAR results from both VBL accumulation and DNM cytotoxicity studies demonstrate that COVO, a steric descriptor indicating solvent accessible volume of a molecule, and HEFO are inversely related to P-gp modulation activity.

In the present study, we have developed QSAR/QSPKR models based on 3D molecular modeling and multivariate statistical analysis to evaluate a series of new compounds having potent *in vitro* P-gp inhibition and minimal calcium channel antagonistic activities. Seven of the synthesized compounds, I_a, I_j, I_k, I_m II_a, II_m, and II_n, were selected for further *in vivo* animal studies based on their prominent P-gp inhibition, negligible Ca^{2+} channel binding activity, and relatively low systemic clearance predicted by our QSPKR models.

The statistical approaches to QSAR/QSPKR used in this investigation can capture the linear relationships between molecular descriptors and biological targets. Because only a limited number of compounds were included in the present study, a larger dataset would be required to validate the current QSAR/QSPKR models. The methodology may facilitate the further integration of QSAR/QSPKR in drug discovery and preclinical development.

ACKNOWLEDGMENTS

The authors thank Dr. Linping Zhang for synthesis of the 1,4-dihydropyridines and pyridines. Supported in part by a grant from the Kapoor Charitable Foundation (SUNY).

REFERENCES

1. P. Borst, R. Evers, M. Kool, and J. Wijnholds. A family of drug transporters: the multidrug resistance-associated proteins. *J. Natl. Cancer Inst.* **92**:1295–1302 (2000).
2. D. R. Ferry, M. A. Russell, and M. H. Cullen. P-glycoprotein possesses a 1,4-dihydropyridine-selective drug acceptor site which is allosterically coupled to a vinca-alkaloid-selective binding site. *Biochem. Biophys. Res. Commun.* **188**:440–445 (1992).
3. G. A. Fisher, B. L. Lum, and B. I. Sikic. The reversal of multidrug resistance. *Cancer Treat. Res.* **78**:45–70 (1995).
4. G. A. Fisherand and B. I. Sikic. Drug resistance in clinical oncology and hematology. Introduction. *Hematol./Oncol. Clin. North Am.* **9**:xi–xii (1995).
5. S. Ekins, R. B. Kim, B. F. Leake, A. H. Dantzig, E. G. Schuetz, L. B. Lan, K. Yasuda, R. L. Shepard, M. A. Winter, J. D. Schuetz, J. H. Wikel, and S. A. Wrighton. Three-dimensional quantitative structure–activity relationships of inhibitors of P-glycoprotein. *Mol. Pharmacol.* **61**:964–973 (2002).
6. I. Pajeva and M. Wiese. Molecular modeling of phenothiazines and related drugs as multidrug resistance modifiers: a comparative molecular field analysis study. *J. Med. Chem.* **41**:1815–1826 (1998).
7. P. H. Van der Graaf, J. Nilsson, E. A. Van Schaick, and M. Danhof. Multivariate quantitative structure–pharmacokinetic relationships (QSPKR) analysis of adenosine A1 receptor agonists in rat. *J. Pharm. Sci.* **88**:306–312 (1999).
8. X. F. Zhou, L. Zhang, E. Tseng, E. A. Scott-Ramsay, J. J. Schentag, R. A. Coburn, and M. E. Morris. New 4-aryl-1,4-dihydropyridines and 4-arylpyridines as P-glycoprotein inhibitors. *Drug Metab. Dispos.* **33**:321–328 (2004).
9. R. Peri. *Regulation of L-Type Calcium Channels in Pituitary GH4C1 Cells by Membrane Depolarization and 1,4-Dihydropyridines*, State University of New York at Buffalo, Buffalo, NY, 1998.
10. D. R. Abernethy and J. B. Schwartz. Pharmacokinetics of calcium antagonists under development. *Clin. Pharmacokinet.* **15**:1–14 (1988).
11. L. Goedhals, W. R. Bezwoda, R. P. Abratt, F. Rathgeb, K. J. Goebel, and W. Wurst. Bioavailability and pharmacokinetic characteristics of dexniguldipine–HCl, a new anticancer drug. *Int. J. Clin. Pharmacol. Ther.* **33**:664–669 (1995).
12. D. E. Mager and W. J. Jusko. Quantitative structure–pharmacokinetic/pharmacodynamic relationships of corticosteroids in man. *J. Pharm. Sci.* **91**:2441–2451 (2002).
13. R. Tobias. *An Introduction to Partial Least Square*, SAS Institute Inc., Cary, NC, 1997.
14. W. M. Meylan and P. H. Howard. Atom/fragment contribution method for estimating octanol–water partition coefficients. *J. Pharm. Sci.* **84**:83–92 (1995).
15. P. Geladi and B. Kowalski. Partial least square regression: a tutorial. *Anal. Chim. Acta* **185**:1–17 (1986).
16. L. Eriksson and E. Johansson. Multivariate design and modeling in QSAR—tutorial. *Chemometr. Intell. Lab. Syst.* **34**:1–19 (1996).
17. M. Mahmoudian and W. G. Richards. QSAR of binding of dihydropyridine-type calcium antagonists to their receptor on ileal smooth muscle preparations. *J. Pharm. Pharmacol.* **38**:272–276 (1986).
18. R. A. Coburn, M. Wierzba, M. J. Suto, A. J. Solo, A. M. Triggle, and D. J. Triggle. 1,4-Dihydropyridine antagonist activities at the calcium channel: a quantitative structure–activity relationship approach. *J. Med. Chem.* **31**:2103–2107 (1988).
19. V. N. Viswanadhan, G. A. Mueller, S. C. Basak, and J. N. Weinstein. Comparison of a neural net-based QSAR algorithm (PCANN) with hologram- and multiple linear regression-based QSAR approaches: application to 1,4-dihydropyridine-based calcium channel antagonists. *J. Chem. Inf. Comput. Sci.* **41**:505–511 (2001).
20. T. Clark. *A Handbook of Computational Chemistry: A Practical Guide to Chemical Structure and Energy Calculations*, Wiley, New York, NY, 1985.
21. K. Fujimura, A. Ota, and Y. Kawashima. Quantitative structure–activity relationships of Ca(2+)-antagonistic semotiadil congeners. *Chem. Pharm. Bull. (Tokyo)* **44**:542–546 (1996).
22. W. A. Catterall, M. J. Seagar, M. Takahashi, and K. Nunoki. Molecular properties of dihydropyridines-sensitive calcium channels. In D. W.-Wray, R. I. Norman, and P. Hess (eds.), *Calcium Channels*, Vol. 560, Annals of the New York Academy of Sciences, New York, 1989, pp. 1–14.
23. K. Palm, P. Stenberg, K. Luthman, and P. Artursson. Polar molecular surface properties predict the intestinal absorption of drugs in humans. *Pharm. Res.* **14**:568–571 (1997).
24. D. F. Veber, S. R. Johnson, H. Y. Cheng, B. R. Smith, K. W. Ward, and K. D. Kopple. Molecular properties that influence the oral bioavailability of drug candidates. *J. Med. Chem.* **45**:2615–2623 (2002).
25. P. Chiba, W. Holzer, M. Landau, G. Bechmann, K. Lorenz, B. Plagens, M. Hitzler, E. Richter, and G. Ecker. Substituted 4-acylpyrazoles and 4-acylpyrazolones: synthesis and multidrug resistance-modulating activity. *J. Med. Chem.* **41**:4001–4011 (1998).